Published by Institute of Physics Publishing for SISSA

Received: *February 13, 2008*
Accepted: *March 6, 2008*
Published: *March 13, 2008*

Time-symmetric initial data of large brane-localized black hole in RS-II model

Norihiro Tanahashi and Takahiro Tanaka

Department of Physics, Kyoto University, Kyoto 606-8502, Japan
E-mail: tanahashi@tap.scphys.kyoto-u.ac.jp, tama@scphys.kyoto-u.ac.jp

Abstract: In the aim of shedding a new light on the classical black hole evaporation conjecture stating that a static brane-localized black hole (BH) larger than the bulk curvature scale does not exist in Randall-Sundrum II (RS-II) model, we investigate time-symmetric initial data with a brane-localized apparent horizon (AH) and analyzed its properties. We find that a three-parameter family of such initial data can be constructed by simply placing a brane on a constant time surface of Schwarzschild anti-de Sitter space. By this method, we unambiguously confirm that initial data with an arbitrarily large AH area do exist. We compare the ADM mass and the horizon area of our initial data with that of the black string (BS) solution. If there is a sequence of static brane-localized BH solutions, such solutions should be contained in the time-symmetric initial data. Moreover, if they are stable, it will have a smaller mass compared with the BS solution with the same horizon area. However, we find that any initial data constructed by this method do not have a smaller mass than the BS solution when the horizon area is larger than the size determined by the bulk curvature scale. We further investigate what kind of configuration realizes the minimum mass for the same AH area. The configuration that realizes the smallest mass turns out to be the one close to the BS truncated by a cap. One may think that this indicates the existence of a static brane-localized BH solution. However, since our three-parameter family of initial data does not include the configuration resembling the BS solution, this minimum of mass may just reflect the expected minimum of mass corresponding to the BS solution. We also demonstrate that the same method applies to construct initial data in (3+1)-dimensional RS-II brane world. In this case an exact solution of a brane-localized BH exists but BS solution does not. Nevertheless, the behavior of the initial data is quite similar in both cases. We find that the known exact solution always has a smaller mass than our initial data with the same horizon area. This result enforces the standard belief that the exact BH solution is the most stable black object in the four-dimensional RS-II model. These results are all consistent with the classical BH evaporation conjecture, but unfortunately it turns out that they do not provide a strong support of it.

Keywords: Large Extra Dimensions, Black Holes.

JHEP03(2008)041

Contents

1. Introduction

The Randall-Sundrum II (RS-II) model [1] is a brane world model, which provides a way to realize our four-dimensional world in a higher-dimensional spacetime requested by the string theory or the M-theory. RS-II model is composed of five-dimensional bulk spacetime with negative cosmological constant and a four-dimensional brane with positive tension. Matter fields are confined on the brane while gravity can propagate through the bulk spacetime. It is known that the weak gravitational field produced by a mass on the brane obeys the usual four-dimensional Newton law with a correction suppressed at a large distance from the source [1 – 5], though the extra-dimension extends infinitely in this model. This fact means that it is difficult to distinguish this model from an ordinary four-dimensional model as long as we investigate the weak gravity regime. Thus we turn focus on the effect of strong gravity. We study the objects formed after gravitational collapse on the brane, in which the effect of strong gravity becomes essential.

Naively, a static black hole (BH) whose horizon is localized near the brane will be formed as a final state of gravitational collapse on the brane. There is an exact static solution with an event horizon, which is black string (BS) [6]. However, it seems unlikely that a BS is formed as a result of gravitational collapse since the BS on the RS-II model is singular and also unstable due to so-called Gregory-Laflamme instability [7]. A static solution of a large BH localized on the brane, however, has not been discovered yet, despite

JHEP03(2008)041

lots of effort on this issue [8 – 16]. Numerical solution of a static brane-localized BH has been constructed when the horizon size is not much larger than the bulk curvature scale, but the construction becomes harder as the horizon size becomes larger [17, 18]. This fact does not exclude the possibility that a static solution of brane-localized BH larger than the bulk curvature scale does exist, but we do not have any strong evidence of its existence. As an explanation of the lack of static solution, there is a conjecture that brane-localized static BHs larger than bulk curvature scale do not exist in RS-II model based on the AdS/CFT correspondence [19, 20].

There are several works related to this conjecture [21 – 29], but no definite conclusion is obtained yet. It is desirable to investigate the possibility of the presence of static black hole solution directly in order to test the validity of this conjecture. However, it is technically difficult to construct a static large brane-localized BH numerically. Thus, we consider time-symmetric initial data which have a brane-localized apparent horizon (AH), expecting that their properties may give some insight into the brane-localized BH. Notice that all static solutions are contained in the time-symmetric initial data.

This paper is organized as follows. We will explain the method how we construct initial data in section 2. We find that a three-parameter family of such initial data can be constructed by simply placing a brane on a constant time surface of Schwarzschild anti-de Sitter (AdS) space. In section 3, using this method, we give an existence proof of initial data with a large AH area. We also compare the ADM mass and the five-dimensional horizon area of our initial data with that of the BS solution. We further investigate what kind of configuration realizes the minimum mass for a given AH area. We also compute the initial data in (3+1)-dimensional RS brane world, in which an exact static solution of brane-localized BH does exist [30, 31]. The results are compared with those in (4+1)-dimensional case. Section 4 is devoted to summary and conclusion.

2. Initial data construction method

In this section we introduce a construction method of time-symmetric initial data with a brane-localized AH in RS-II model. The model is composed of two copies of five-dimensional empty bulk with negative cosmological constant Λ separated by a $\mathbb{Z}_2$-symmetric positive tension brane. The tension of the brane satisfies the RS condition $\lambda = 3k/4\pi G_5$ with $k = \sqrt{-\Lambda/6}$, where G_5 is the five-dimensional gravitational constant. The setup is compatible with a Minkowski brane with AdS bulk with the bulk curvature length being k^{-1}. The initial data we consider have $O(3)$-symmetry in the spacelike dimension as well as the symmetry with respect to time reversal. These symmetries are property shared with static brane-localized BH solutions. Hence, we think it appropriate to restrict our attention to this class of initial data.

In order to obtain a time-symmetric initial data of the RS-II model, we have to solve the Hamiltonian constraint equation in the bulk and on the brane simultaneously. In this paper, we do that by taking a constant time slice from a known vacuum solution with cosmological constant. We use five-dimensional AdS (topological) BH solutions as such solutions. By using the bulk metric taken from a known solution, the constraint equations in the bulk

JHEP03(2008)041

are automatically satisfied. In this spacetime we can find spacelike minimal hypersurfaces on a constant time slice, on which the expansion Θ of out-going null geodesic congruence vanishes. Even if those minimal hypersurfaces are not closed, they are candidates of the AH. By cutting this spacetime with a pure-tension brane with $\mathbb{Z}_2$-symmetry, a part of AH candidate, even if they are not closed originally, can be reformed into a trapped surface. In placing a momentarily static brane with $\mathbb{Z}_2$-symmetry, we solve the brane configuration starting from a point on a $\Theta = 0$ hypersurface so as to satisfy the Hamiltonian constraint on the brane. In this manner we obtain a family of initial data with an AH localized on the brane. We note here that this construction method is similar to that used in ref. [32] to generate a solution of a static brane with brane-localized matter.

2.1 Bulk solution

The starting point of our construction procedure is to choose an asymptotically AdS vacuum solution of the Einstein equations with negative cosmological constant Λ. In this study, we use the well-known AdS Schwarzschild (the case with $\beta = +1$ below) solution and its extensions (the cases with $\beta = 0$ and -1 below), which are called "topological BH in AdS" [33]. The metric is given by

$$ds^2 = -U(r)dt^2 + \frac{dr^2}{U(r)} + r^2\sigma_{IJ}(x)dx^I dx^J, \tag{2.1}$$

where

$$U(r) = \beta + k^2 r^2 - \frac{\mu}{r^2} \quad (\beta = +1, 0, -1),$$

and

$$\sigma_{IJ}(x)dx^I dx^J = \begin{cases} d\chi^2 + \sin^2\chi d\Omega_{\rm II}^2 & (\beta = +1) \\ d\chi^2 + \chi^2 d\Omega_{\rm II}^2 & (\beta = 0) \\ d\chi^2 + \sinh^2\chi d\Omega_{\rm II}^2 & (\beta = -1) \end{cases}$$

are the metrics on the three-dimensional maximally symmetric spaces. Here μ is the mass parameter and $d\Omega_{\rm II}^2 = d\theta^2 + \sin^2\theta\, d\phi^2$. We can see that the spacetime (2.1) is asymptotically AdS, since the term $k^2 r^2$ in $U(r)$ dominates at $r \to \infty$.

The spacetime described by this metric with $\beta = +1$ has an spherical event horizon at $r = r_g$ where $U(r)$ vanishes. Also in the other two cases ($\beta = 0$ and -1), $r = r_g$ defined by $U(r_g) = 0$ becomes a surface on which the expansion Θ of the outgoing null geodesic congruence vanishes. However, these surfaces are not closed unless we assume non-trivial identification in the maximally symmetric three space. Nevertheless, we refer to the surface defined by $r = r_g$ as an event horizon in all three cases. The three spatial metric on the horizon is flat for $\beta = 0$ while it is hyperbolic for $\beta = -1$. Notice that the event horizon does not exist in the case of $\mu < 0$ for $\beta = 0, +1$, and in the case of $\mu < -1/4k^2$ for $\beta = -1$. We refer to these solutions as spherical ($\beta = +1$), flat ($\beta = 0$) and hyperbolic ($\beta = -1$) AdS BHs, respectively, in this paper.

The AdS BH solutions are connected to each other via the flat one. Both spherical and hyperbolic AdS BHs reduce to the flat one in the limit $\mu \to \infty$. This can be made

transparent by the following coordinate rescaling:

$$\bar{t} = \left(k^2\mu\right)^{1/4} t, \quad \bar{r} = \left(k^2\mu\right)^{-1/4} r, \quad \bar{\chi} = \left(k^2\mu\right)^{1/4} \chi. \tag{2.2}$$

Then, the metric for $\beta = \pm 1$ in the limit $\mu \to \infty$ becomes

$$ds^2 \xrightarrow{\mu\to\infty} -\left(k^2\bar{r}^2 - \frac{1}{k^2\bar{r}^2}\right) d\bar{t}^2 + \left(k^2\bar{r}^2 - \frac{1}{k^2\bar{r}^2}\right)^{-1} d\bar{r}^2 + \bar{r}^2\left(d\bar{\chi}^2 + \bar{\chi}^2 d\Omega_{\rm II}\right). \tag{2.3}$$

This is nothing but the metric for $\beta = 0$ after the rescaling (2.2). In this expression μ is not present any more. This means that the flat AdS BH has only one free parameter k.

In the following discussion we set k to unity by rescaling the unit of length. In this sense, this background spacetime has only one free parameter μ, which becomes one of free parameters of the initial data we construct below.

2.2 AH candidates in AdS BH spacetime

Let us consider a three surface on a t =constant hypersurface Σ_t. If the expansion Θ of the outgoing null geodesic congruence on this three-surface vanishes, it becomes a candidate of an AH. Even if the surface is not closed in the original spacetime, it might be made compact after we introduce a $\mathbb{Z}_2$-symmetric brane. Hence, we refer to such a surface with $\Theta = 0$ as an apparent horizon candidate (AHC).

We denote the unit vector normal to an AHC in Σ_t as s^i. Here Latin indices starting from the middle of the alphabet $(i, j, \ldots)$ run over all spatial coordinates. Then the condition of vanishing expansion of the outgoing null geodesic congruence emanating from this AHC is given by

$$K - K_{ij}s^i s^j - D_i s^i = 0, \tag{2.4}$$

where K_{ij} is the extrinsic curvature of the surface Σ_t and K is its trace. D_i is the covariant differentiation with respect to the induced metric on Σ_t. Since we have $K_{ij} = 0$ by the assumption of time-symmetric initial data, this equation is reduced to

$$D_i s^i = 0, \tag{2.5}$$

which determines the position of the AHC.

Assuming $O(3)$-symmetry of AHC, we specify its trajectory by $(r, \chi) = (r_{\rm AH}(\zeta), \chi_{\rm AH}(\zeta))$, where ζ is the proper radial length along the AHC measured from the axis of the $O(3)$-symmetry. These $r_{\rm AH}(\zeta)$ and $\chi_{\rm AH}(\zeta)$ satisfy

$$U^{-1} r'^2_{\rm AH} + r^2_{\rm AH}\, \chi'^2_{\rm AH} = 1, \tag{2.6}$$

where a prime means a differentiation with respect to the argument, which is ζ here. Then, the spacelike unit vector normal to the AHC is

$$s_\mu = \frac{r_{\rm AH}}{\sqrt{U}}\left(\chi'_{\rm AH}, -r'_{\rm AH}\right). \tag{2.7}$$

JHEP03(2008)041

Then eq. (2.5) and eq. (2.6) can be recasted into a set of two ordinary differential equations, whose explicit form for the spherical AdS BH bulk is given by

$$\frac{\sqrt{U}r_{\rm AH}}{r'_{\rm AH}}\chi''_{\rm AH}+4\sqrt{U}\chi'_{\rm AH}-\frac{2\cot\chi_{\rm AH}}{\sqrt{U}r_{\rm AH}}r'_{\rm AH}=0,$$
$$-\frac{1}{\sqrt{U}r_{\rm AH}\chi'_{\rm AH}}r''_{\rm AH}+3\sqrt{U}\chi'_{\rm AH}+\frac{r'_{\rm AH}}{2U^{3/2}r_{\rm AH}\chi'_{\rm AH}}\left(\frac{dU}{dr}r'_{\rm AH}-4U\chi'_{\rm AH}\cot\chi_{\rm AH}\right)=0. \quad (2.8)$$

The expression for the hyperbolic AdS BH bulk is obtained by simply replacing $\cot\chi_{\rm AH}$ with $\coth\chi_{\rm AH}$.

We solve this equation setting $\chi_{\rm AH}(0)=0$. We can freely choose the value of $r_{\rm AH}(0)$, which specifies the position of the AHC in the background spacetime. This $r_0^{\rm AH}\equiv r_{\rm AH}(0)$ becomes one of free parameters of the initial data we construct. The boundary condition at $\zeta=0$ is given by

$$r'_{\rm AH}(0)=0, \quad (2.9)$$

which comes from the regularity of the AHC on the axis. We solve eq. (2.8) with this boundary condition numerically to obtain the trajectories of AHCs.

2.3 Brane trajectory

Next we put a vacuum brane with $\mathbb{Z}_2$-symmetry in the AdS BH bulk. We denote the unit normal of the brane by $\tilde{s}_\mu$. We take this $\tilde{s}_\mu$ in the direction toward the bulk from the brane. We introduce the induced metric $\tilde{\gamma}_{\mu\nu}\equiv g_{\mu\nu}-\tilde{s}_\mu\tilde{s}_\nu$ on the brane. The extrinsic curvature $\tilde{K}_{ab}$ on the brane is defined by $\tilde{K}_{ab}=-\tilde{\gamma}_a{}^\mu\tilde{\gamma}_b{}^\nu\nabla_\mu\tilde{s}_\nu$. Here Latin indices starting from the beginning of the alphabet $(a,b,\ldots)$ run the four-dimensional coordinates on the brane.

A vacuum brane has the four-dimensional energy-momentum tensor localized on the brane given by

$$T_{ab}=-\lambda\tilde{\gamma}_{ab}. \quad (2.10)$$

Israel's junction condition [34] on the brane is given by

$$\tilde{K}_{ab}-\tilde{K}\tilde{\gamma}_{ab}=\frac{1}{2}\cdot 8\pi G_5 T_{ab}, \quad (2.11)$$

where we used $\mathbb{Z}_2$-symmetry across the brane. This junction condition is just a part of the Einstein equations integrated across the brane. The equations for the initial data to satisfy is the constraint equations, i.e., the (t,t)- and (t,i)-components of the Einstein equations. They are the Hamiltonian constraint and momentum constraints respectively. Since the momentum constraints are trivially satisfied at the moment of the time-reversal symmetry, we only have to consider the Hamiltonian constraint, which is (t,t)-component of eq. (2.11). Using the normal vector $\tilde{s}^\mu$, this condition is written as

$$D_i\tilde{s}^i=-3k. \quad (2.12)$$

As before, we assume $O(3)$-symmetry, and we specify the brane trajectory by $(r,\chi)=(r_b(\xi),\chi_b(\xi))$, where ξ is the proper radial length along the brane. The spacelike unit

normal $\tilde{s}_\mu$ is given by eq. (2.7), replacing $r_{\rm AH}$ and $\chi_{\rm AH}$ with r_b and χ_b respectively. Then the Hamiltonian constraint (2.12) becomes a second order ODE of $r_b(\xi)$ and $\chi_b(\xi)$. The explicit expression for the spherical AdS BH becomes eq. (2.8), replacing $r_{\rm AH}$ and $\chi_{\rm AH}$ with r_b and χ_b on the left hand sides, and 0 with $-3k$ on the right hand sides.

As we are not interested in the spacetime interior of the AHC, we solve the brane trajectory from a point on the AHC. The choice of the starting point on the AHC is arbitrary. This degree of freedom becomes one of free parameters of the initial data we construct. The boundary condition for eq. (2.12) at this point is determined by the regularity of the AH across the brane. Namely, the AH should intersect the brane perpendicularly, i.e. $\tilde{s}_\mu s^\mu = 0$. This leads to the condition,

$$(r_b', \chi_b') = \left(\sqrt{U} r_{\rm AH}\, \chi_{\rm AH}', -\frac{r_{\rm AH}'}{\sqrt{U} r_{\rm AH}}\right), \tag{2.13}$$

at the crossing point. We solve eq. (2.12) numerically to obtain the brane trajectory. Once the AHC is truncated by the brane, it becomes a closed surface with vanishing expansion, $\Theta = 0$. However, the AH is not simply a compact surface with $\Theta = 0$ but it must be the outermost one among such surfaces. Thus we have to check if there is no other $\Theta = 0$ hypersurface in the region outside of the AHC. If such surfaces exist, the outermost one is the true AH. This true AH search can be done by the shooting method. We take a point on the axis at $\chi = 0$, and we extend the hypersurface with $\Theta = 0$ from the point perpendicularly to the axis. This hypersurface may hit the brane at an angle. Moving the starting point on the axis, we search for the case that the hypersurface with $\Theta = 0$ crosses the brane perpendicularly. If there is no such a hypersurface with $\Theta = 0$, the original AHC is the genuine AH. In the case that true AH exists outside AHC, such initial data will be also given by other values of free parameters in the parameter space. Hence, we just discard such initial data, and analyze only the data which have no outer AH.

In the case that no event horizon exists in the original bulk solution, the original spacetime has a naked curvature singularity at $r = 0$, at which the Kretschmann scalar diverges as $\mathcal{O}(\mu^2/r^8)$. However, even in this case, AH may be formed after a brane is placed. Then, this singularity cannot be seen from an observer outside the horizon if the brane and the AH hide the singularity. In this case there is no problem in adopting this singular bulk to construct initial data. Nevertheless, we do not consider this case in the following discussion simply because such initial data do not show any interesting properties as a matter of fact.

2.4 ADM mass and AH area

To characterize the initial data constructed by the method explained above, we discuss how to extract the ADM mass measured on the brane and the AH area.

The ADM mass measured on the brane is calculated from the spatial part of the induced metric on the brane,

$$d\tilde{l}^2 = \left(\frac{d\rho_b}{d\xi}\right)^{-2} d\rho_b^2 + \rho_b^2 d\Omega_{\rm II}^2, \tag{2.14}$$

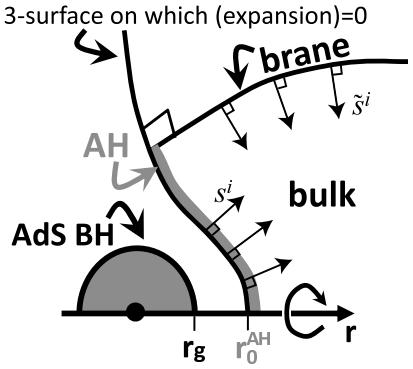

Figure 1: A schematic picture of the initial data that we construct. The whole initial data is composed by gluing two copies of the portion presented in this figure together along the brane. This initial data has three degrees of freedom: the mass parameter μ of the AdS BH, the position of the AH on the axis $r = r_0^{\rm AH}$ and the position of the brane starting point. For convenience, we take the AH area, $A_{\rm AH}$, in place of the last parameter.

where we introduced a new radial coordinate $\rho_b(\xi) \equiv r_b(\xi) \sin \chi_b(\xi)$ for the spherical AdS BH background case, corresponding to the circumferential radius of (θ, ϕ)-two sphere. For the hyperbolic AdS BH case, $\sin \chi_b$ in ρ_b is replaced with $\sinh \chi_b$.

Asymptotically, ρ_b' behaves as

$$\rho_b' \approx 1 - \frac{\tilde{G}_4 M_{\rm ADM}}{\xi} + \cdots , \tag{2.15}$$

where $M_{\rm ADM}$ is the four-dimensional ADM mass and $\tilde{G}_4 = kG_5$ is the effective four-dimensional Newton constant. In order to determine $M_{\rm ADM}$ accurately, $r_b(\xi)$ and $\chi_b(\xi)$ must be solved up to a large enough ξ. In the present method, which only requires to solve the constraint equation along the brane trajectory, we do not have to solve the Hamiltonian constraint equation in the bulk. This enables us to determine $\rho_b(\xi)$ up to very large ξ. This is an advantage of this method.

The AH area is also an important physical quantity, which plays an important role in the following discussion. The spatial part of the induced metric on the AH is

$$\sigma^{\rm AH}_{IJ} dx^I dx^J = d\zeta^2 + \rho_{\rm AH}(\zeta)^2 d\Omega_{\rm II}^2 \tag{2.16}$$

in the spherical AdS BH case, where $\rho_{\rm AH}(\zeta) \equiv r_{\rm AH}(\zeta) \sin \chi_{\rm AH}(\zeta)$. For the hyperbolic AdS BH background case, $\sin \chi_{\rm AH}$ in this expression is replaced with $\sinh \chi_{\rm AH}$. Then the area of the AH, $A_{\rm AH}$, is calculated as

$$A_{\rm AH} = \int \sqrt{\sigma^{\rm AH}} d\chi d\theta d\varphi = 2 \int_0^{\zeta_0} 4\pi \, {\rho_{\rm AH}}^2 \, d\zeta, \tag{2.17}$$

where ζ_0 is the value of ζ at which the brane crosses the AH.

JHEP03(2008)041

3. Analysis of the properties of initial data

3.1 Existence of initial data with a large AH

The family of initial data constructed by the method explained above has three free parameters: the mass parameter of the AdS BH bulk μ, the position of the starting point of AH $r_0^{\rm AH}$ and the location of the brane starting point. We will use the area of the AH, $A_{\rm AH}$, instead of the last parameter. We do not count the bulk curvature length scale k^{-1} as a parameter since we can absorb it by rescaling the unit of length. Since there is no static brane-localized BH solution with a large horizon area, one may suspect that time-symmetric initial data with a large AH do not exist. However, we found no difficulty in constructing initial data with a large AH.

As we mentioned above, the original AHC may not be a true AH if another AH is found outside of it. When we fix one of three free parameters, we still have two remaining free parameters. In figure 2 and 3, the parameter regions in which another AH is found outside of the original AHC are shaded, and those in which the brane is not asymptotically flat are dotted. We refer to the shaded and dotted regions as the excluded regions. The excluded region is confined to the region where $r_0^{\rm AH}$ is close to the BH horizon of the original AdS BH irrespective of the size of $A_{\rm AH}$.

3.2 Area comparison with RS-II black string

The only known exact solution containing a black object in the RS-II model is the BS solution. The BS solution in the RS-II model is given by

$$ds^2 = \frac{1}{k^2 z^2}\left(-f(r)dt^2 + f(r)^{-1}dr^2 + r^2 d\Omega_{\rm II}^2 + dz^2\right), \tag{3.1}$$

where $f(r) = 1 - r_g/r$ and r_g is the horizon radius on the brane. r_g is related to the ADM mass measured on the brane as $M_{\rm BS} = r_g/2\tilde{G}_4$. The brane is at $z = k^{-1}$ in these coordinates. The area of the BS horizon $A_{\rm BS}$ is

$$A_{\rm BS} = 2\int_{k^{-1}}^{\infty} \frac{4\pi r_g^2}{(kz)^3}\, dz = 4\pi r_g^2 k^{-1}. \tag{3.2}$$

We compare this area with the AH area $A_{\rm AH}$ in the initial data, equating $M_{\rm ADM}$ of the initial data to $M_{\rm BS}$.

What we want to know is whether one can construct initial data with a larger horizon area than BS when the ADM mass is fixed. Why is it an interesting question? If there is a static localized BH solution, it gives a time-symmetric initial data. Suppose that there is a static localized BH solution. Then, if we can survey all possible time-symmetric initial data, the static solution must be found among them. Moreover, if the solution is stable, we expect that it will realize the maximum horizon area among all configurations with the same mass. Hence, its horizon area must be greater than that of BS, too. Hence, if we find

JHEP03(2008)041

a time-symmetric initial data that has the horizon area larger than BS, it suggests that there is a static brane-localized BH solution.[1]

Now we show the results of the comparison between $A_{\rm AH}$ and $A_{\rm BS}$. In figure 2, we show the boundaries in the parameter space between two cases, $A_{\rm AH} < A_{\rm BS}$ and $A_{\rm AH} > A_{\rm BS}$. For the purpose of display, we reduced the parameter space to two dimensions by fixing the value of μ. The boundary curves are drawn in the parameter space $\left((r_0^{\rm AH} - r_g)/r_g, A_{\rm AH}\right)$ for several values of μ.

The panel (a) shows the border lines of the two regions for $\mu = 1.8 \times 10^{-1} k^{-2}$, $1.9 \times 10^{-2} k^{-2}$ and $1.0 \times 10^{-3} k^{-2}$, while the panel (b) for $\mu = 1.7 k^{-2}$, $1.5 \times 10^{1} k^{-2}$ and $1.4 \times 10^{2} k^{-2}$ in the case of the spherical AdS BH background. In the panel (a) the region $(r_0^{\rm AH} - r_g)/r_g < 10^{-3}$ is not shown since the boundary is mostly inside the excluded region. We found that the boundaries are at around $A_{\rm AH} \sim \mathcal{O}(k^{-3})$ irrespective of the value of μ and $\left(r_0^{\rm AH} - r_g\right)/r_g$. The panels (c) and (d) are the figures in the case of the hyperbolic AdS BH background for $\mu = (-1/4 + 10^{-2})k^{-2}$ and $\mu = 10 k^{-2}$. In the gray region the AH area is larger than the BS horizon area. The initial data in the shaded region have an outer AH and they are excluded from the data set to conduct the horizon area comparison. We found that the AH area never becomes larger than the BS area when $A_{\rm AH} \gtrsim \mathcal{O}(k^{-3})$ even in this case. Namely, all the initial data that we can construct by the present method have a horizon area smaller than that of BS with the same ADM mass if the AH area is larger than a typical size determined by the bulk curvature scale. This result is consistent with the classical BH evaporation conjecture, though it does not exclude the existence of counter-examples.

3.3 Initial data with maximum horizon area for a fixed mass

As we stated above, if there is a static brane-localized BH solution, it must be contained in time-symmetric initial data, if we take into account all possible configurations. Moreover, if the solution is stable, we expect that it will be realized as a maximum of the horizon area among all time-symmetric initial data with the same ADM mass. Although we can search only a limited part of time-symmetric initial data by our method, it will be still interesting to see which configuration realizes the maximum horizon area when the ADM mass is fixed.

Technically, it is easier to fix the AH area than to fix the ADM mass, because $A_{\rm AH}$ itself is one of the three parameters that label our initial data. To the contrary, in order to calculate $M_{\rm ADM}$, the information in the asymptotic region $r \to \infty$ is needed. The initial data that realizes the maximum horizon area with the ADM mass fixed should have the

[1] Of course, our statement here is naive. Even if there are initial data with the horizon area larger than BS, we cannot claim that it proves the existence of a static brane-localized BH solution. One possible loophole is that such initial data may not evolve into a stationary state. One may point out that the configuration that realizes the maximum of the horizon area for a fixed ADM mass will exist. Such a configuration seems to be static. This statement might be true, but we would not be able to deny the possibility that such a configuration might be singular. In fact, if all time-symmetric initial data have a smaller horizon area than that of the BS solution, the maximum of the horizon area is realized by the BS solution, which is singular. All the initial data close to BS will be unstable due to the Gregory-Laflamme instability, and they will not settle into a regular stationary state.

JHEP03(2008)041

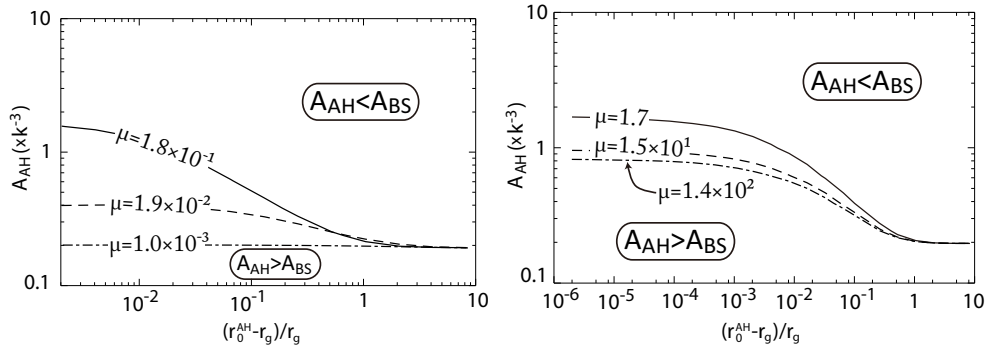

(a) Spherical AdS BH background, $\mu < \mathcal{O}(k^{-2})$

(b) Spherical AdS BH background, $\mu > \mathcal{O}(k^{-2})$

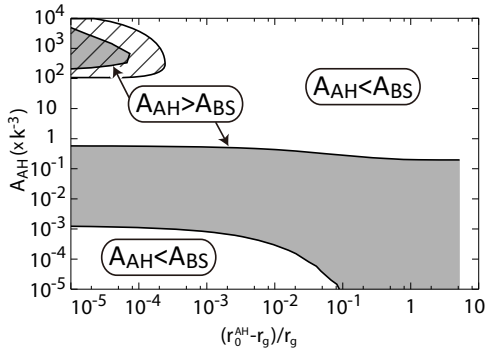

(c) Hyperbolic AdS BH background, $\mu = (-1/4 + 10^{-2})k^{-2}$

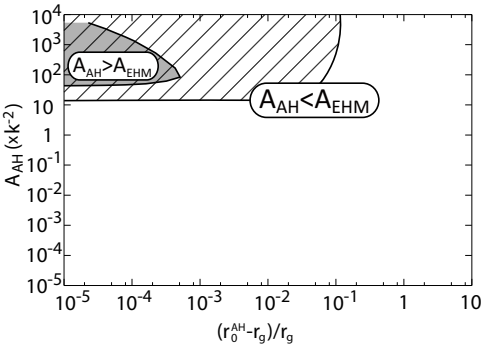

(d) Hyperbolic AdS BH background, $\mu = 10k^{-2}$

Figure 2: The boundaries between two cases, $A_{\rm AH} < A_{\rm BS}$ and $A_{\rm AH} > A_{\rm BS}$, are shown for several values of μ. The horizontal axis $(r_0^{\rm AH} - r_g)/r_g$, which is the distance between the AH and the event horizon of AdS BH normalized by r_g. The vertical axis is the AH area. The AH area is larger (smaller) than the BS horizon area below (above) the boundary curve. The panels (a) and (b) are the figures in the case of the spherical AdS BH background for $\mu < \mathcal{O}(k^{-2})$ and $\mu > \mathcal{O}(k^{-2})$ respectively. The region $(r_0^{\rm AH} - r_g)/r_g < 10^{-3}$ is not shown in the panel (a), because the boundary is mostly inside the excluded region. The panels (c) and (d) are the figures in the case of the hyperbolic AdS BH background for $\mu = (-1/4 + 10^{-2})k^2$ and $\mu = 10k^{-2}$. In the gray region the AH area is larger than the BS horizon area. The initial data in the shaded region have an outer AH and they must be excluded from the data set to conduct the horizon area comparison.

minimum ADM mass when the AH area is fixed. Therefore we fix the AH area and search for the initial data of the minimum ADM mass varying the other parameters, μ and $r_0^{\rm AH}$.

We have drawn contour plots of $M_{\rm ADM}/M_{\rm BS}$ for several values of $A_{\rm AH}$ in figure 3, where $M_{\rm BS}$ is the ADM mass of a BS whose horizon area is equal to $A_{\rm AH}$. Different plots correspond to different values of the fixed AH area. The left (right) half of each plot corresponds to the initial data which have the spherical (hyperbolic) AdS BH bulk. Here we should remember that the shaded and dotted regions should be neglected because there is a true AH outside the original AHC. Once we exclude these regions, we find that there is one and only one minimum of $M_{\rm ADM}$ in all contour plots.

We found that the mass minimum is realized on the spherical AdS BH side when

JHEP03(2008)041

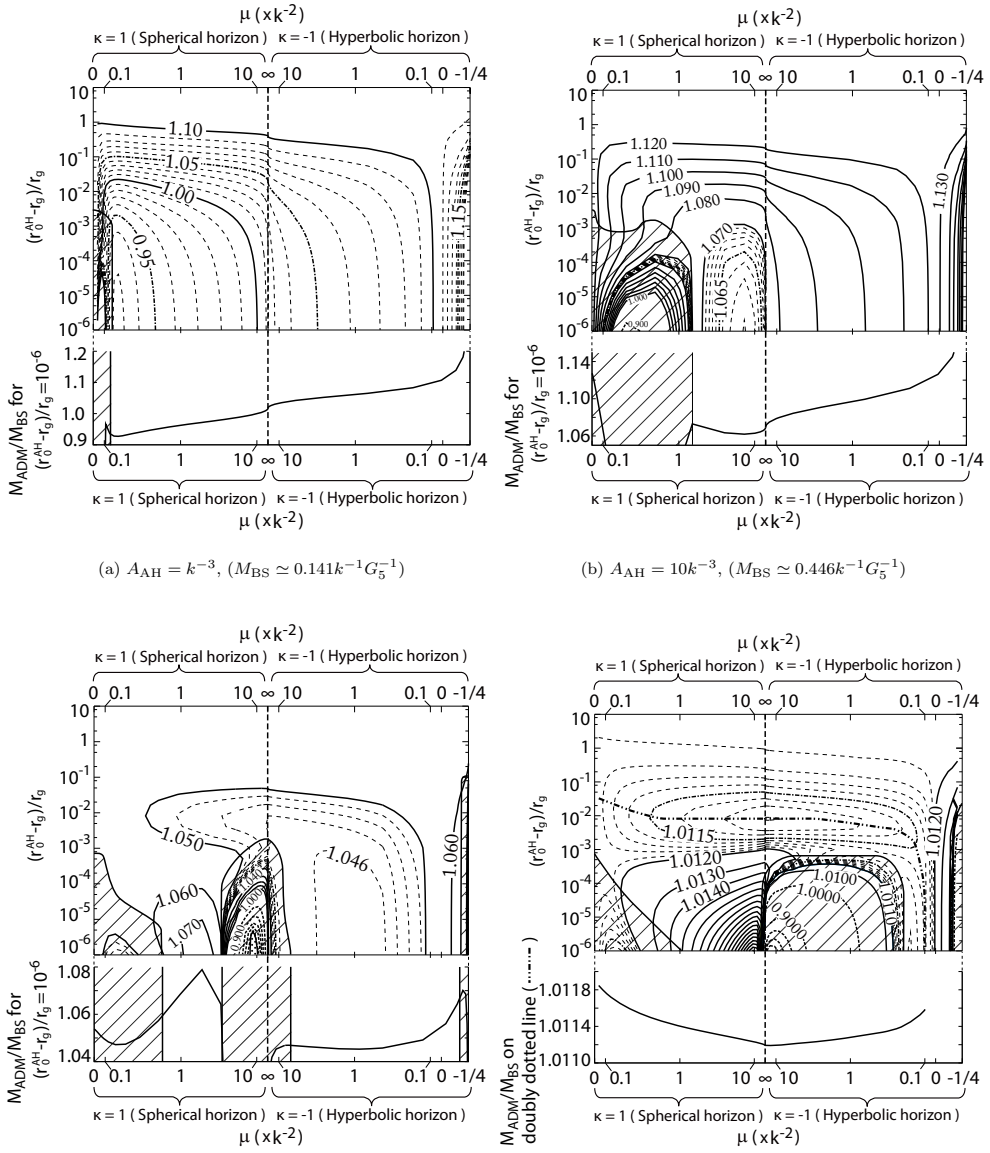

(a) $A_{\rm AH} = k^{-3}$, $(M_{\rm BS} \simeq 0.141 k^{-1} G_5^{-1})$

(b) $A_{\rm AH} = 10k^{-3}$, $(M_{\rm BS} \simeq 0.446 k^{-1} G_5^{-1})$

(c) $A_{\rm AH} = 10^2 k^{-3}$ $(M_{\rm BS} \simeq 1.41 k^{-1} G_5^{-1})$

(d) $A_{\rm AH} = 10^3 k^{-3}$ $(M_{\rm BS} \simeq 4.46 k^{-1} G_5^{-1})$

Figure 3: The contour plots of $M_{\rm ADM}/M_{\rm BS}$ on the parameter space $\left(\mu, (r_0^{\rm AH} - r_g)/r_g\right)$ for several values of $A_{\rm AH}$, where $M_{\rm BS}$ is the ADM mass of BS whose horizon area is equal to $A_{\rm AH}$. The horizontal axis is the value of μ for the spherical and hyperbolic AdS BH cases. The curves below the contour plots show the values of $M_{\rm ADM}$ for $(r_0^{\rm AH} - r_g)/r_g = 10^{-6}$ in the panels (a), (b) and (c), and the value along the doubly dotted curve drawn in the contour plot in the panel (d). The initial data in the shaded region have an outer AH and they are excluded from the search for the mass minimum. For the parameters in the dotted region in the panel (c), the initial data do not have an asymptotically flat brane, so they are also excluded from the data set. The mass minimum is realized on the spherical AdS BH background in the panel (a) and (b), on the hyperbolic AdS BH background in the panel (c), and on the flat AdS BH background in the panel (d).

$A_{\rm AH}$ is smaller than a typical scale determined by the bulk curvature scale, i.e. when $A_{\rm AH} \lesssim k^{-3}$. The minimum seemed to be realized in the limit $r_0^{\rm AH} \to r_g$ in this regime. As

JHEP03(2008)041

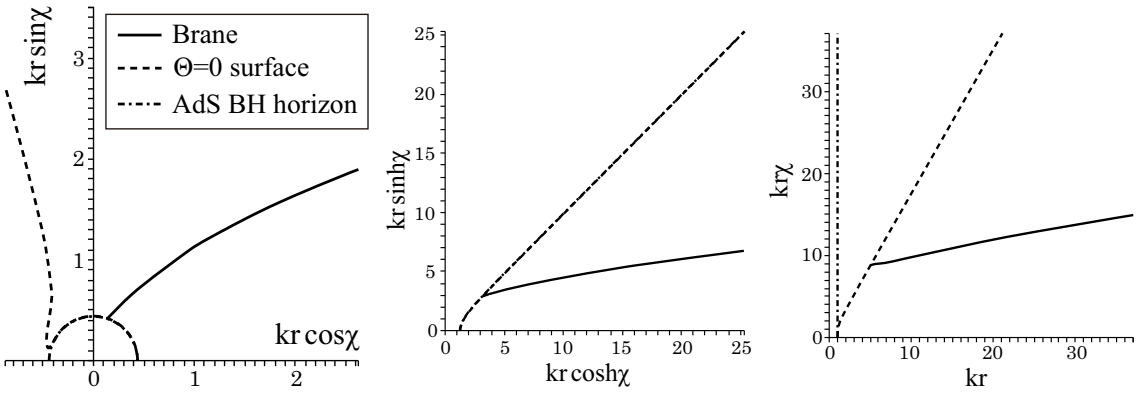

(a) $A_{\rm AH} = k^{-3}$ (b) $A_{\rm AH} = 10^2 k^{-3}$ (c) $A_{\rm AH} = 10^3 k^{-3}$

Figure 4: The configurations of the AH and the brane in the AdS BH bulk for $A_{\rm AH} = k^{-3}, 10^2 k^{-3}$ and $10^3 k^{-3}$. The event horizon of the AdS BH bulk is also drawn. The type of the AdS BH bulk is different in each plot, i.e. spherical, hyperbolic and flat, respectively, in the increasing order of $A_{\rm AH}$.

$A_{\rm AH}$ is increased, the location of the minimum moves toward the hyperbolic AdS BH side. When $r_0^{\rm AH} \approx r_g$, AH is very close to the event horizon of the AdS BH bulk. If we further increase $A_{\rm AH}$, $r_0^{\rm AH}$ at the mass minimum leaves r_g and the minimum is realized in the limit $\mu \to \infty$, in which the bulk becomes the flat AdS BH spacetime. In this regime the AH deviates from the event horizon of the AdS BH bulk. We displayed the trajectories of the AH and the brane for the initial data with the minimum ADM mass for three typical values of $A_{\rm AH}$ in figure 4.

When we consider a brane-localized BH which is small compared to the bulk curvature scale k^{-1}, the effect of brane tension is negligible. Then we have an initial data which has the brane placed on the equatorial plane of the AdS BH is approximately a static solution, at least, near the horizon. Thus such an initial data will have the minimum ADM mass among the configurations of the same AH area. Our result completely agrees with this expectation.

When the AH is large, the bulk curvature effect becomes large. Then, five-dimensional AdS BH with the brane on its equatorial plane is no longer close to a static configuration. In order to study the character of the initial data that realizes the minimum ADM mass when $A_{\rm AH} \gg k^{-3}$, we computed the scalar curvature ${}^{(3)}R_{\rm AH}$ of the induced three metric on the AH. We plot ${}^{(3)}R_{\rm AH}$ against $\rho_{\rm AH}$, the circumferential radius of (θ, ϕ)-two sphere, (normalized by the bulk curvature length) in figure 5. We found that ${}^{(3)}R_{\rm AH}$ is negative everywhere on the AH and the value stays very close to $-6k^2$ near the brane. Significant deviation from $-6k^2$ occurs only for a small circumferential radius ($\rho \lesssim k^{-1}$).

We compare the above result with the intrinsic curvature of the three metric on the BS horizon,

$$ {}^{(3)}R_{\rm BS} = 2\left(\frac{1}{\rho^2} - 3k^2\right). \tag{3.3} $$

When $\rho \gtrsim k^{-1}$, we have ${}^{(3)}R_{\rm BS} \approx -6k^2$. This behavior is very similar to the initial data that minimizes the mass. Thus we find that the AH geometry of our initial data is close

JHEP03(2008)041

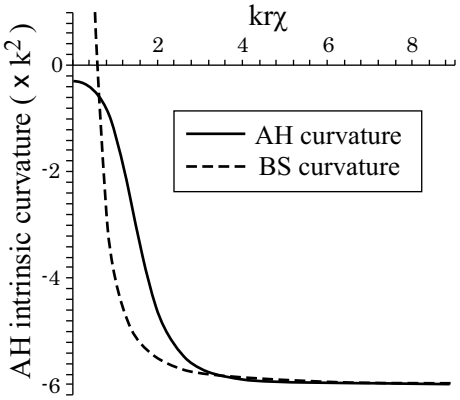

Figure 5: The intrinsic curvature of the induced three metric on the AH for the initial data shown in figure 4(c). The dashed line shows the value of the intrinsic curvature of the BS horizon whose area is equal to $10^3 k^{-3}$.

to the horizon geometry of the BS solution near the brane.

Since BS is an exact static solution, it will give a local or the global minimum of the ADM mass for a given AH area. Therefore there will be a dip with respect to the mass around the BS configuration in the complete parameter space of all possible time-symmetric initial data. However, we are not here investigating all possible configurations of time-symmetric initial data. Our parameter space is very restricted. In fact, the BS configuration is not contained in our initial data. Then, in the regime $A_{\rm AH} \gtrsim k^{-3}$, the minimum of the ADM mass in our present two-dimensional parameter space may correspond to the dip around the BS configuration. This is a scenario consistent with the conjecture that there is no static large brane-localized BH. However, it is also possible that the mass minimum that we found corresponds to a dip associated with another static brane-localized BH solution.

It will be interesting to point out that we can construct initial data with AH starting with the pure AdS bulk. This corresponds to the case of $\mu = 0$ on the hyperbolic AdS BH side. This case is not in the excluded region of the parameter space. (On the spherical AdS BH side, r_g behaves like $\approx \sqrt{\mu}$ in the limit $\mu \to 0$. Thus, in figure 3 the location of the starting point of the AHC, $r_0^{\rm AH}$, is always close to the horizon in this limit. Therefore $\mu = 0$ does not simply correspond to the case of the pure AdS bulk. On the other hand, we have $r_g \approx k^{-1}$ in the limit $\mu \to 0$ on the hyperbolic AdS BH side. Thus, the effect of non-zero μ on the AHC vanishes in the limit $\mu \to 0$.) If we solve eq. (2.8) for $\mu = 0$, the AHC becomes homogeneous hyperbolic space, as shown in figure 4, with intrinsic curvature being ${}^{(3)}R_{\rm AH} = -6k^2$. Its behavior is close to BS for $\rho \gtrsim k^{-1}$, but the deviation from BS for $\rho \lesssim k^{-1}$ is larger compared with the initial data which minimizes the ADM mass.

4. Four-dimensional case

In this section we analyze the brane-localized BH initial data in four-dimensional RS-II model in a parallel manner. The bulk cosmological constant is $\Lambda = -3k^2$ and the brane tension is $\lambda = 2k/4\pi G_4$, where G_4 is the four-dimensional gravitational constant. In

JHEP03(2008)041

the four-dimensional case the situation looks quite different from the higher-dimensional models. The counterpart of the analytic BS solution discussed in section 3.2 does not exist. Instead, there exists an exact solution of a brane-localized BH [30, 31]. Therefore the properties of the initial data might be different from the five-dimensional case.

As the bulk spacetime, we consider the four-dimensional AdS BH solution

$$ds^2 = -\,\mathrm{U}(r)dt^2 + \frac{dr^2}{\mathrm{U}(r)} + r^2\tilde{\sigma}_{IJ}(x)dx^I dx^J, \tag{4.1}$$

where

$$\mathrm{U}(r) = \beta + k^2 r^2 - \frac{\mu}{r},$$

and

$$\tilde{\sigma}_{ij}(x)dx^i dx^j = \begin{cases} d\chi^2 + \sin^2\chi d\theta^2 & (\beta = +1)\,, \\ d\chi^2 + \chi^2 d\theta^2 & (\beta = 0)\,, \\ d\chi^2 + \sinh^2\chi d\theta^2 & (\beta = -1)\ . \end{cases}$$

The properties of this solution is similar to the five-dimensional case. The rescaling corresponding to eqs. (2.2) in the present case is given by

$$\bar{t} = (k\mu)^{1/3}\, t, \quad \bar{r} = (k\mu)^{-1/3}\, r, \quad \bar{\chi} = (k\mu)^{1/3}\, \chi. \tag{4.2}$$

The equation that determines the AHC (2.5) becomes

$$\begin{aligned} &\frac{\sqrt{U}r_{\mathrm{AH}}}{r'_{\mathrm{AH}}}\chi''_{\mathrm{AH}} + 3\sqrt{U}\chi'_{\mathrm{AH}} - \frac{\cot\chi_{\mathrm{AH}}}{\sqrt{U}r_{\mathrm{AH}}}r'_{\mathrm{AH}} = 0, \\ &-\frac{1}{\sqrt{U}r_{\mathrm{AH}}\chi'_{\mathrm{AH}}}r''_{\mathrm{AH}} + 2\sqrt{U}\chi'_{\mathrm{AH}} + \frac{r'_{\mathrm{AH}}}{2U^{3/2}r_{\mathrm{AH}}\chi'_{\mathrm{AH}}}\left(\frac{dU}{dr}r'_{\mathrm{AH}} - 2U\chi'_{\mathrm{AH}}\cot\chi_{\mathrm{AH}}\right) = 0. \end{aligned} \tag{4.3}$$

The Hamiltonian constraint on the brane (2.12) is given by eq. (4.3), replacing $r_{\mathrm{AH}}(\zeta)$ and $\chi_{\mathrm{AH}}(\zeta)$ with $r_b(\xi)$ and $\chi_b(\xi)$ on the left hand sides, and 0 with $-2k$ on the right hand sides. The area of the AH is given by

$${}^{(4)}A_{\mathrm{AH}} = 2\int_0^{\zeta_0} 2\pi\rho_{\mathrm{AH}}\, d\zeta. \tag{4.4}$$

On the three-dimensional brane, the mass of an object is given by

$$M_3 = \frac{\delta\phi}{4\pi k G_4}, \tag{4.5}$$

where $\delta\phi$ is the deficit angle in the asymptotic region on the brane. Notice that $kG_4/2$ is the three-dimensional effective Newton constant on the brane. The asymptotic deficit angle $\delta\phi$ is obtained from the relationship between the proper length in the radial direction ξ, and the circumferential radius ρ_b as

$$d\rho_b = (2\pi - \delta\phi)d\xi. \tag{4.6}$$

JHEP03(2008)041

Thus, the explicit formula for M_3 is

$$M_3 = \frac{1}{2kG_4} \lim_{\xi\to\infty} \left(1 - \rho_b'\right). \tag{4.7}$$

The analysis of the initial data goes in parallel to the five-dimensional case presented in section 3. In the five-dimensional case we used the BS solution as a reference. As mentioned above, in the four-dimensional RS-II brane world a similar analytic BS solution does not exist, but there is an exact solution of the brane-localized BH found by Emparan, Horowitz and Myers [30] (EHM). Here we briefly review the property of this exact solution.

The bulk of the solution is given by a special case of the AdS C-metric [35]

$$ds^2 = \frac{1}{k^2(x-y)^2}\left[-F(y)dt^2 + \frac{dy^2}{F(y)} + \frac{dx^2}{G(x)} + G(x)d\phi^2\right], \tag{4.8}$$

where $F(y) = y^2 + 2\bar{\mu}y^3$ and $G(x) = 1 - x^2 - 2\bar{\mu}x^3$. This metric has a BH horizon at $y = y_{\rm hor} \equiv -1/2\bar{\mu}$. Basically the coordinate y is the radial coordinate, and x is an angular coordinate. In the case of $\bar{\mu} > 0$, $G(x) = 0$ has three roots. We denote the largest positive root by x_2. We take the region specified by $0 \le x \le x_2$ and $-1/2\mu \le y \le x$ as the bulk. The $\mathbb{Z}_2$-symmetric brane is located at $x = 0$. Then the junction condition across the brane is satisfied. The axis of ϕ-rotation is at $x = x_2$. To avoid the conical singularity on this axis, the periodicity of ϕ should be chosen as

$$\Delta\phi = \frac{4\pi}{|G'(x_2)|} = \frac{2\pi}{x_2\left(1 + 3\bar{\mu}x_2\right)}\,. \tag{4.9}$$

Thus, the horizon area of the EHM solution is given by

$$A_{\rm EHM} = 2\Delta\phi \int_0^{x_2} \frac{dx}{k^2(x - y_{\rm hor})^2} = \frac{16\pi\bar{\mu}^2}{k^2(1+3\bar{\mu}x_2)(1+2\bar{\mu}x_2)}. \tag{4.10}$$

It is good to consider the limiting cases, $\bar{\mu} \ll 1$ and $\bar{\mu} \gg 1$, to understand the behavior of $A_{\rm EHM}$. When $\bar{\mu} \ll 1$, x_2 and $A_{\rm EHM}$ are approximated as

$$x_2 \simeq 1 - \bar{\mu}, \qquad A_{\rm EHM} \simeq 16\pi\bar{\mu}^2 k^{-2}. \tag{4.11}$$

When $\bar{\mu} \gg 1$, x_2 and $A_{\rm AH}$ are approximately given by

$$x_2 \simeq (2\bar{\mu})^{-1/3}\,, \qquad A_{\rm EHM} \simeq \frac{8\pi}{3k^2}\,(2\bar{\mu})^{2/3}\,. \tag{4.12}$$

The mass M_3 measured on the brane is proportional to the asymptotic deficit angle $\delta\phi$ as given in eq. (4.5). Since the induced metric on the brane becomes

$$d\tilde{s}^2 = -\left(1 + \frac{2\bar{\mu}}{r}\right)d\bar{t}^2 + \frac{1}{1 + \frac{2\bar{\mu}}{r}}dr^2 + r^2 d\phi^2, \tag{4.13}$$

where we introduced $\bar{t} \equiv k^{-1}t$ and $r \equiv 1/ky$, we find that the deficit angle is simply given by $\delta\phi = 2\pi - \Delta\phi$. Hence, we have

$$M_3 = \frac{1}{2kG_4}(1 - F), \tag{4.14}$$

with $F \equiv \Delta\phi/2\pi = x_2^{-1}(1+3\bar{\mu}x_2)^{-1}$. Using $F = 1 - 2kG_4M_3$, the area of the EHM solution (4.10) can be expressed as

$$A_{\rm EHM} = \frac{16\pi}{9k^2}\frac{\left(-2+\sqrt{1+3F^2}\right)^2}{-1+\sqrt{1+3F^2}}. \tag{4.15}$$

We can easily relate the mass and the horizon area of the EHM BH solution by using the formulas (4.14) and (4.15).

We can also calculate the intrinsic curvature of the two-dimensional metric on the event horizon as

$${}^{(2)}R_{\rm EHM} = \frac{k^2}{2\bar{\mu}^2}\left\{8\left(\bar{\mu}x\right)^3 + 12\left(\bar{\mu}x\right)^2 + 6\left(\bar{\mu}x\right) - 4\bar{\mu}^2 + 1\right\}, \tag{4.16}$$

and x is related to the radius of the circle in the ϕ-direction, ρ, as

$$\rho = \frac{\sqrt{G(x)}}{k(x-y_{\rm hor})}\frac{\Delta\phi}{2\pi} = \frac{2\bar{\mu}}{k}\frac{\sqrt{1-x^2-2\bar{\mu}x^2}}{x_2(1+3\bar{\mu}x_2)(1+2\bar{\mu}x)}.$$

Figure 6 shows the parameter region in which the AH area becomes larger than the horizon area of the EHM solution with the same mass. We found that the whole parameter region in which the AH area becomes larger than the horizon area of the EHM solution is in the excluded region. This result is consistent with the naive expectation that the EHM solution is the most stable black object in the four-dimensional RS-II model and hence that any other black objects, even if they exist, have smaller horizon size.

In figure 7 we show the plots of the mass normalized by the mass of the EHM solution of the same horizon area, which are parallel to figure 3 of the five-dimensional case. We found that the behavior of the contour plot is similar to that of the five-dimensional case. When we vary the value of the AH area, the location of the mass minimum changes exactly in the same way as in the previous case.

We show the configurations of the branes and AHs for the initial data of the mass minimum for a few fixed values of $A_{\rm AH}$ in figure 8. The shape of the brane and the AH is also similar to the five-dimensional case. In figure 9 we plot the intrinsic curvature on the AH for $A_{\rm AH} = 10^2k^{-2}$ by the solid curve. The counterpart in the EHM solution is also shown in the same plot.

The interpretation of these results goes almost parallel to the five-dimensional case. The difference appears when the AH area is large. We consider the BS solution as a reference in the five-dimensional case, while the EHM solution in the four-dimensional case. The behavior of these two solutions look quite different at first sight. The horizon of the BS solution extends infinitely, while that of the EHM solution is finite. However, if we compare the intrinsic curvature of the horizon of these two exact solutions shown in figure 5 and figure 9, the behavior is quite similar except for the region where the circumferential radius ρ is small compared with the bulk curvature length scale k^{-1}.

JHEP03(2008)041

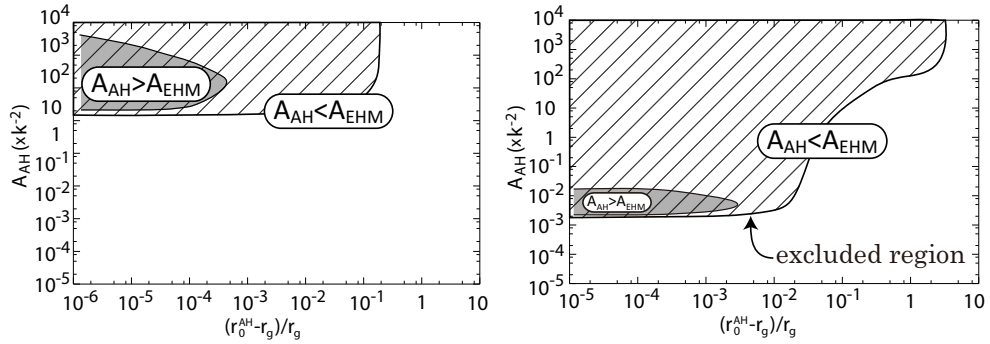

(a) Spherical AdS BH background, $\mu = 10^{-2}k^{-1}$

(b) Spherical AdS BH background, $\mu = 10k^{-1}$

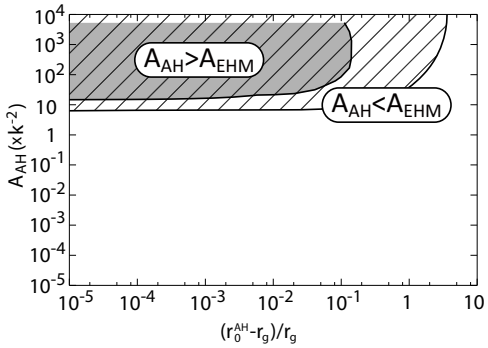

(c) Hyperbolic AdS BH background, $\mu = (-2/3^{3/2} + 10^{-2})k^{-1}$

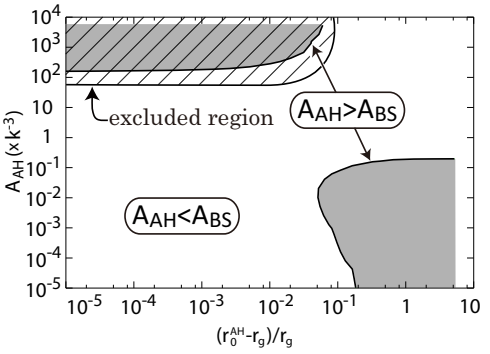

(d) Hyperbolic AdS BH background, $\mu = 10k^{-1}$

Figure 6: The result of area comparison between the AH in the initial data and the EHM solution for $\mu = 10^{-2}k^{-1}$ and $10k^{-1}$ in the spherical AdS BH background case, and $\mu = (-2/3^{3/2}+10^{-2})k^{-1}$ and $10k^{-1}$ in the hyperbolic AdS BH background case. The AH area of the initial data is larger than the horizon area of the EHM solution for the parameters in the gray regions in the plots, and in the other regions the horizon area of the EHM solution is larger. The shaded regions are excluded from the analysis because the initial data in these regions have outer AHs. For any μ, the gray region is covered by a shaded region. It means that the horizon area of the EHM solution is larger than the AH area of the initial data for any parameters.

5. Discussion

In order to have an insight into the black objects with a large horizon radius in the model of warped extra-dimension, we studied time-symmetric initial data of RS-II model in five and four-dimensions. We constructed three-parameter family of time-symmetric initial data with a brane-localized AH, by placing a $\mathbb{Z}_2$-symmetric brane in the AdS Schwarzschild bulk. We have shown that one can construct initial data with an arbitrarily large AH area. Our method of constructing the initial data requires just solving ordinary differential equations. Hence, the conclusion that initial data with an arbitrarily large AH area exist is quite robust.

In the five-dimensional model the area of the obtained initial data was always smaller than the event horizon area of the BS solution whose mass is as large as the initial data

JHEP03(2008)041

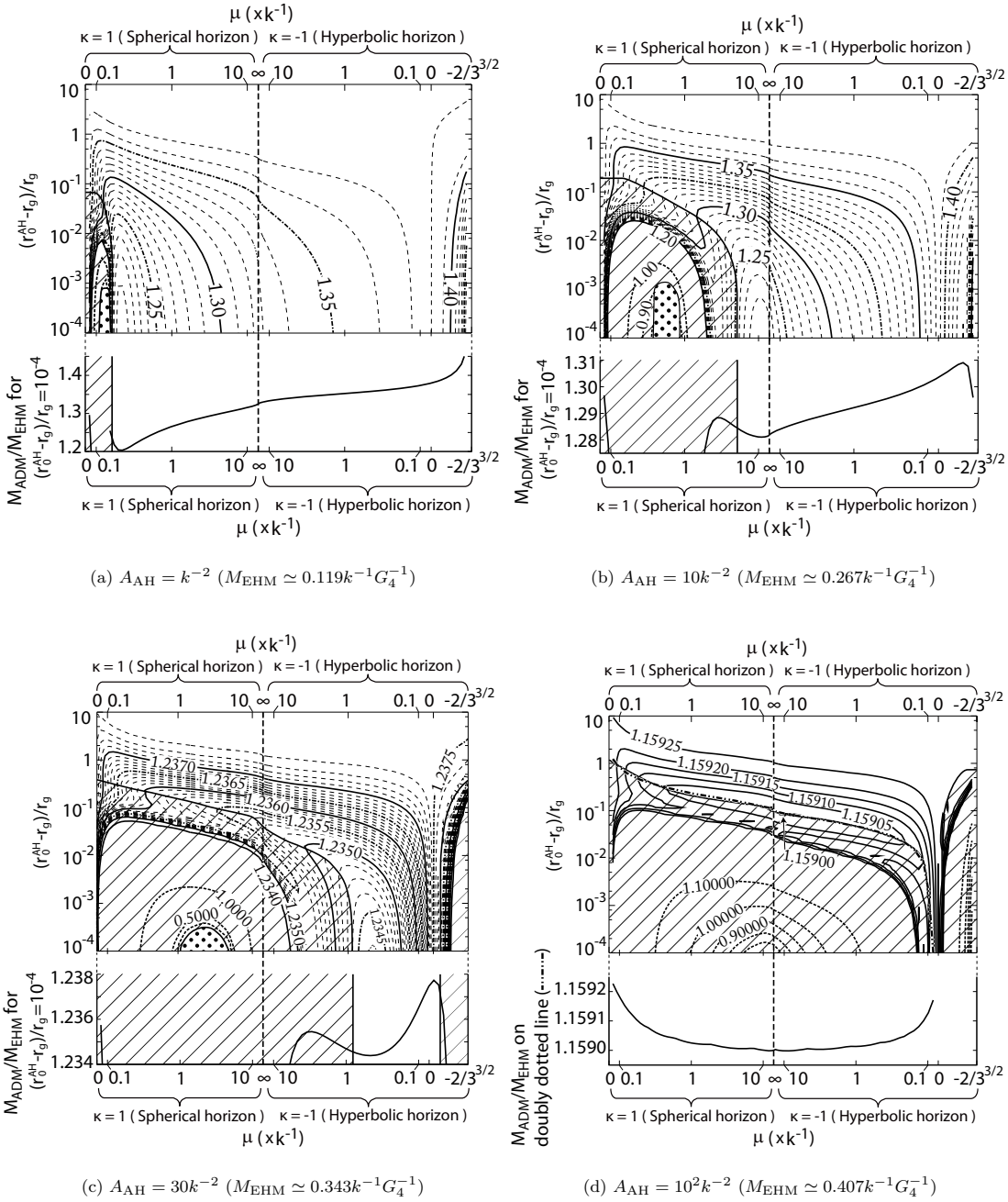

(a) $A_{\rm AH} = k^{-2}$ ($M_{\rm EHM} \simeq 0.119 k^{-1} G_4^{-1}$)

(b) $A_{\rm AH} = 10k^{-2}$ ($M_{\rm EHM} \simeq 0.267 k^{-1} G_4^{-1}$)

(c) $A_{\rm AH} = 30k^{-2}$ ($M_{\rm EHM} \simeq 0.343 k^{-1} G_4^{-1}$)

(d) $A_{\rm AH} = 10^2 k^{-2}$ ($M_{\rm EHM} \simeq 0.407 k^{-1} G_4^{-1}$)

Figure 7: The contour plots of $M_{\rm ADM}/M_{\rm EHM}$ in the four-dimensional case, where $M_{\rm EHM}$ is the mass of the EHM BH whose horizon area is equal to $A_{\rm AH}$. The curves below the contour plots in the panels (a), (b) and (c) show the values of the ADM mass for $(r_0^{\rm AH} - r_g)/r_g = 10^{-4}$, and the curve in the panel (d) shows the value along the doubly dotted curve in the contour plot.

when the horizon area is sufficiently large compared to the bulk curvature length cubed. In the following sense, this result is consistent with the scenario that these initial data evolve into configurations similar to BS, which is unstable through Gregory-Laflamme instability. The event horizon, which must exist outside the AH area, should have a

JHEP03(2008)041

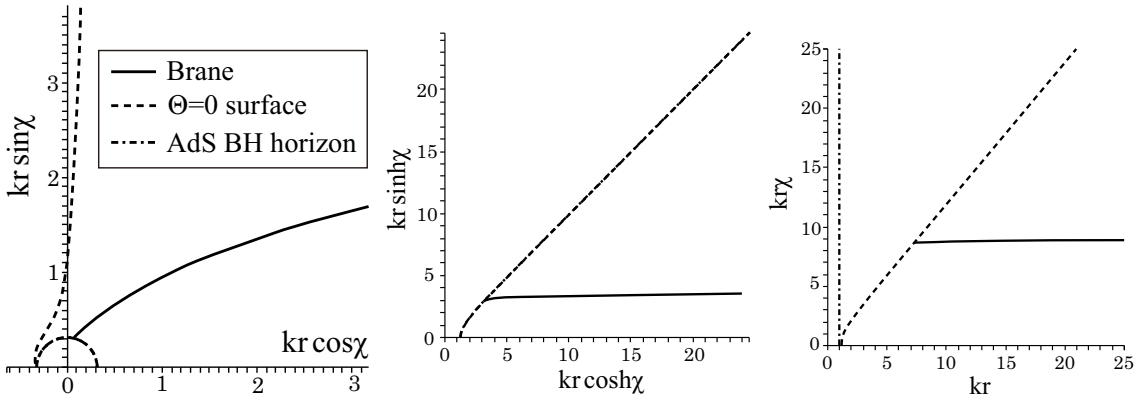

(a) $A_{\rm AH} = k^{-2}$ (b) $A_{\rm AH} = 30k^{-2}$ (c) $A_{\rm AH} = 10^2 k^{-2}$

Figure 8: The configuration of the initial data with the minimum mass for a few values of $A_{\rm AH}$. The bulk metrics of these plots are spherical, hyperbolic and flat AdS BHs, respectively.

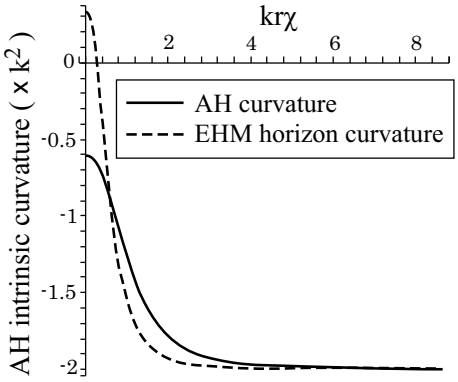

Figure 9: ${}^{(2)}R_{\rm AH}$ of the the AH in the panel (c) in figure 8. The counterpart in the EHM solution is also shown by the dashed line.

larger area than AH. The area theorem tells that the area of the event horizon does not decrease as a course of time evolution, while the mass will not increase when there is no incoming energy flux from infinity. Hence, if there is an initial data whose horizon area is significantly larger than that of BS with the same mass, such an initial data cannot evolve into the configuration close to BS.

We also explored the initial data that realizes the minimum mass with the AH area fixed, which is expected to be the closest to a static solution. We found that the initial data that realizes the minimum mass is close to the spherical AdS BH with a brane on its equatorial plane when the AH area is small, while it is close to BS when the AH area is large.

We conducted the same analysis also in the case of four-dimensional bulk spacetime since the situation looks quite different in this case. The BS solution does not exist, but we have an exact brane-localized BH solution found by Emparan, Horowitz and Myers (EHM), instead. Nevertheless, the results of the analyses as to the time-symmetric initial data were quite similar to the five-dimensional case. We found that the area of the initial data is always larger than the EHM solution with the same mass, which is in harmony

JHEP03(2008)041

with the naive expectation that the EHM solution is the most stable black object in four-dimensional RS-II model.

Unfortunately, the analysis presented in this paper did not provide a strong indication about the classical evaporation conjecture because the initial data that we examined were very limited. However, it is a remarkable progress that we have shown that time-symmetric initial data with a large AH area can be constructed. As a next step, we can consider the time evolution of these initial data. The family of initial data we constructed in this study will be a good starting point for researches in this direction.

Acknowledgments

TT is supported by Monbukagakusho Grant-in-Aid for Scientific Research Nos. 17340075 and 19540285. This work is also supported in part by the 21st Century COE "Center for Diversity and Universality in Physics" at Kyoto university, from the Ministry of Education, Culture, Sports, Science and Technology of Japan. The authors thank Takashi Nakamura, Shuichiro Yokoyama and Keisuke Izumi for useful comments.

References

[1] L. Randall and R. Sundrum, *An alternative to compactification*, *Phys. Rev. Lett.* **83** (1999) 4690 [hep-th/9906064].

[2] J. Garriga and T. Tanaka, *Gravity in the brane-world*, *Phys. Rev. Lett.* **84** (2000) 2778 [hep-th/9911055].

[3] T. Wiseman, *Relativistic stars in Randall-Sundrum gravity*, *Phys. Rev.* **D 65** (2002) 124007 [hep-th/0111057].

[4] I. Giannakis and H.-c. Ren, *Recovery of the Schwarzschild metric in theories with localized gravity beyond linear order*, *Phys. Rev.* **D 63** (2001) 024001 [hep-th/0007053].

[5] H. Kudoh and T. Tanaka, *Second order perturbations in the Randall-Sundrum infinite brane-world model*, *Phys. Rev.* **D 64** (2001) 084022 [hep-th/0104049].

[6] A. Chamblin, S.W. Hawking and H.S. Reall, *Brane-world black holes*, *Phys. Rev.* **D 61** (2000) 065007 [hep-th/9909205].

[7] R. Gregory, *Black string instabilities in anti-de Sitter space*, *Class. and Quant. Grav.* **17** (2000) L125 [hep-th/0004101].

[8] P. Kanti and K. Tamvakis, *Quest for localized 4D black holes in brane worlds*, *Phys. Rev.* **D 65** (2002) 084010 [hep-th/0110298].

[9] D. Karasik, C. Sahabandu, P. Suranyi and L.C.R. Wijewardhana, *Small (1 TeV) black holes in Randall-Sundrum I scenario*, *Phys. Rev.* **D 69** (2004) 064022 [gr-qc/0309076].

[10] D. Karasik, C. Sahabandu, P. Suranyi and L.C.R. Wijewardhana, *Small black holes on branes: is the horizon regular or singular?*, *Phys. Rev.* **D 70** (2004) 064007 [gr-qc/0404015].

[11] N. Dadhich, R. Maartens, P. Papadopoulos and V. Rezania, *Black holes on the brane*, *Phys. Lett.* **B 487** (2000) 1 [hep-th/0003061].

[12] R. Casadio, A. Fabbri and L. Mazzacurati, *New black holes in the brane-world?*, *Phys. Rev.* **D 65** (2002) 084040 [gr-qc/0111072].

[13] A. Chamblin, H.S. Reall, H.-a. Shinkai and T. Shiromizu, *Charged brane-world black holes*, *Phys. Rev.* **D 63** (2001) 064015 [hep-th/0008177].

[14] T. Shiromizu and M. Shibata, *Black holes in the brane world: time symmetric initial data*, *Phys. Rev.* **D 62** (2000) 127502 [hep-th/0007203].

[15] G. Kofinas, E. Papantonopoulos and V. Zamarias, *Black hole solutions in braneworlds with induced gravity*, *Phys. Rev.* **D 66** (2002) 104028 [hep-th/0208207].

[16] R. Casadio and L. Mazzacurati, *Bulk shape of brane-world black holes*, *Mod. Phys. Lett.* **A 18** (2003) 651 [gr-qc/0205129].

[17] H. Kudoh, T. Tanaka and T. Nakamura, *Small localized black holes in braneworld: formulation and numerical method*, *Phys. Rev.* **D 68** (2003) 024035 [gr-qc/0301089].

[18] H. Kudoh, 6-*dimensional localized black holes: numerical solutions*, *Phys. Rev.* **D 69** (2004) 104019 [*Erratum ibid.* **D 70** (2004) 029901] [hep-th/0401229].

[19] T. Tanaka, *Classical black hole evaporation in Randall-Sundrum infinite braneworld*, *Prog. Theor. Phys. Suppl.* **148** (2003) 307 [gr-qc/0203082].

[20] R. Emparan, A. Fabbri and N. Kaloper, *Quantum black holes as holograms in AdS braneworlds*, *JHEP* **08** (2002) 043 [hep-th/0206155].

[21] R. Casadio and C. Germani, *Gravitational collapse and black hole evolution: do holographic black holes eventually 'anti-evaporate'?*, *Prog. Theor. Phys.* **114** (2005) 23 [hep-th/0407191].

[22] P.R. Anderson, R. Balbinot and A. Fabbri, *Cutoff AdS/CFT duality and the quest for braneworld black holes*, *Phys. Rev. Lett.* **94** (2005) 061301 [hep-th/0410034].

[23] C. Galfard, C. Germani and A. Ishibashi, *Asymptotically AdS brane black holes*, *Phys. Rev.* **D 73** (2006) 064014 [hep-th/0512001].

[24] A. Fabbri, S. Farese, J. Navarro-Salas, G.J. Olmo and H. Sanchis-Alepuz, *Semiclassical zero-temperature corrections to Schwarzschild spacetime and holography*, *Phys. Rev.* **D 73** (2006) 104023 [hep-th/0512167].

[25] N. Kaloper and D. Kiley, *Exact black holes and gravitational shockwaves on codimension-2 branes*, *JHEP* **03** (2006) 077 [hep-th/0601110].

[26] A.L. Fitzpatrick, L. Randall and T. Wiseman, *On the existence and dynamics of braneworld black holes*, *JHEP* **11** (2006) 033 [hep-th/0608208].

[27] A. Fabbri and G.P. Procopio, *Quantum effects in black holes from the Schwarzschild black string?*, *Class. and Quant. Grav.* **24** (2007) 5371 [arXiv:0704.3728].

[28] A. Fabbri and G.P. Procopio, *The holographic interpretation of Hawking radiation*, arXiv:0705.3363.

[29] T. Tanaka, *Implication of classical black hole evaporation conjecture to floating black holes*, arXiv:0709.3674.

[30] R. Emparan, G.T. Horowitz and R.C. Myers, *Exact description of black holes on branes*, *JHEP* **01** (2000) 007 [hep-th/9911043].

JHEP03(2008)041

[31] R. Emparan, G.T. Horowitz and R.C. Myers, *Exact description of black holes on branes. II: comparison with BTZ black holes and black strings*, *JHEP* **01** (2000) 021 [hep-th/9912135].

[32] S. Creek, R. Gregory, P. Kanti and B. Mistry, *Braneworld stars and black holes*, *Class. and Quant. Grav.* **23** (2006) 6633 [hep-th/0606006].

[33] D. Birmingham, *Topological black holes in anti-de Sitter space*, *Class. and Quant. Grav.* **16** (1999) 1197 [hep-th/9808032].

[34] W. Israel, *Singular hypersurfaces and thin shells in general relativity*, *Nuovo Cim.* **B44S10** (1966) 1 [*Erratum ibid.* **B 48** (1967) 463].

[35] J.F. Plebanski and M. Demianski, *Rotating, charged, and uniformly accelerating mass in general relativity*, *Ann. Phys. (NY)* **98** (1976) 98.

JHEP03(2008)041